3-27-2018

Upregulation Of Microglial Zeb1 Ameliorates Brain Damage After Acute Ischemic Stroke

Daojing Li

Wenjing Lang

Chen Zhou

Chao Wu

Fang Zhang

See next page for additional authors

Article

Cell Reports

Upregulation of Microglial ZEB1 Ameliorates Brain Damage after Acute Ischemic Stroke

Graphical Abstract

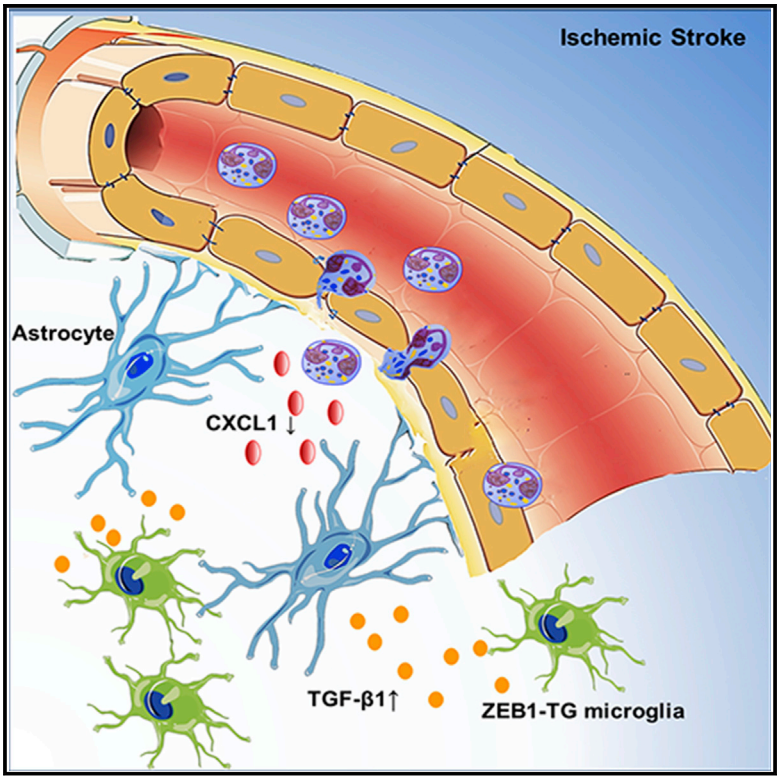

Authors

Daojing Li, Wenjing Lang, Chen Zhou, ..., Qiang Liu, Shuang Yang, Junwei Hao

Correspondence

yangshuang@nankai.edu.cn (S.Y.), hjw@tmu.edu.cn (J.H.)

In Brief

Li et al. show that ZEB1 overexpression mediates microglia responses and, in turn, inhibits production of astrocytic CXCL1 through the TGF-β1-dependent pathway. Reduced CXCL1 leads to the decline of neutrophil infiltration into the brain. This demonstrates the importance of ZEB1 in microglia-orchestrated neuroinflammation and suggests a potential means for reducing stroke-induced neurological injury.

Highlights

- Microglial ZEB1 is upregulated after acute brain ischemia induced by tMCAO
- Targeted overexpression of microglial ZEB1 reduces acute ischemic brain injury
- Microglial ZEB1 regulates the immune response in the CNS after ischemic stroke
- Microglia ZEB1 inhibits the CXCL1 secretion from astrocytes through TGF-β1 pathway

Data and Software Availability

GSE110141

Li et al., 2018, Cell Reports 22, 3574–3586
March 27, 2018
https://doi.org/10.1016/j.celrep.2018.03.011

CellPress

OPEN ACCESS
CellPress

Cell Reports
Article

Upregulation of Microglial ZEB1 Ameliorates Brain Damage after Acute Ischemic Stroke

Daojing Li,[1] Wenjing Lang,[1] Chen Zhou,[2] Chao Wu,[3] Fang Zhang,[1] Qiang Liu,[1,4] Shuang Yang,[3,*] and Junwei Hao[1,5,*]
[1]Department of Neurology, Tianjin Neurological Institute, Tianjin Medical University General Hospital, Tianjin 300052, China
[2]Department of Neurology, Tianjin Huanhu Hospital, Tianjin 300350, China
[3]Department of Medical Genetics, Tianjin Key Laboratory of Tumor Microenvironment and Neurovascular Regulation, Medical College of Nankai University, Tianjin 300071, China
[4]Department of Neurology, Barrow Neurological Institute, St. Joseph's Hospital and Medical Center, Phoenix, AZ 85013, USA
[5]Lead Contact
*Correspondence: yangshuang@nankai.edu.cn (S.Y.), hjw@tmu.edu.cn (J.H.)
https://doi.org/10.1016/j.celrep.2018.03.011

SUMMARY

Microglia are a key immune-competent cell type that respond to environmental and physiological changes during ischemic stroke. However, the molecular mechanisms controlling post-ischemic microglia activity are unclear. Understanding these mechanisms may ultimately reduce disease burden and allow the manipulation of microglia responses to shape the outcomes of stroke. Here, we report that, after experimentally induced stroke, ZEB1 is highly expressed in ipsilateral cerebral hemisphere, where it is upregulated mainly in microglia. Using a conditional transgenic mouse, we found that ZEB1 upregulation in microglia regulates immune responses in the CNS and alleviates brain injury after ischemic stroke. Our data indicate that ZEB1 overexpression mediates microglia responses and, in turn, inhibits the production of astrocytic CXCL1 through the TGF-β1-dependent pathway. Reduced CXCL1 leads to a decline in neutrophil infiltration into the brain, thereby reducing CNS inflammation. Our results demonstrate the importance of ZEB1 in microglia-orchestrated neuroinflammation and suggest a potential means for reducing stroke-induced neurological injury.

INTRODUCTION

Stroke is a major cause of adult disability and death worldwide (Iadecola and Anrather, 2011; Macrez et al., 2011). Inflammation and lymphocyte invasion occur within minutes to a few hours after acute ischemic stroke and are known as key contributors to brain injury (Benakis et al., 2015; Chamorro et al., 2016; Kleinschnitz et al., 2013). Therapeutic interventions that involve manipulating the immune system are being explored in patients with ischemic stroke (Fu et al., 2014, 2015). However, our understanding of immunomodulation is still in its infancy, largely because clinical trials of regulatory drugs have not been generally successful. Also, limited knowledge about the molecular mechanisms underlying neuroinflammation has impeded researchers from better understanding the profound role that inflammation plays in stroke and its aftermath.

Microglia are brain-resident immune cells that refine synaptic networks, promote cellular apoptosis, remove apoptotic cell corpses, position neurons within the developing mammalian barrel cortices, and govern the precise secretion of growth factors for neuronal survival (Parkhurst et al., 2013; Stevens et al., 2007). Depending on the timing and disease stage, microglia also contribute to post-ischemic stroke brain injury or are involved in repairing it. However, the molecular machinery governing post-ischemic microglia activity is complex and far from understood (Hu et al., 2015).

Zinc finger E-box binding homeobox 1 (ZEB1) is a member of the zinc finger-homeodomain transcription factor family that modulates cell differentiation and specific cellular functions in multiple tissues (Funahashi et al., 1993; Hasuwa et al., 2013). In solid tumors, ZEB1 can repress E-cadherin, induce epithelial-mesenchymal transition (EMT), induce chemo- and radioresistant phenotypes, and promote the generation of cancer stem cells (Chaffer et al., 2013; Zhang et al., 2014). ZEB1 also participates in regulating the development of the immune system (Arnold et al., 2012). A previous study reported that ZEB1 overexpression represents a protective response to brain ischemia (Bui et al., 2009), but the cellular and molecular mechanisms of ZEB1 that underlie this protective response against ischemic stroke remain obscure.

Here, we report on the development of a genetic system for targeting microglia that illuminates their pathologic activities during ischemic stroke more specifically and directly than previously possible (Goldmann et al., 2013). To genetically manipulate microglia, we exploit their longevity and self-renewal properties and the expression of Cre recombinase driven by the *CX3CR1* promoter. Using this modified genetic system, we measured ZEB1 expression after brain ischemia and determined the impact of microglial ZEB1 expression on CNS inflammation and tissue injury after stroke. The net effect of microglial ZEB1 signaling is probably determined by moderating the

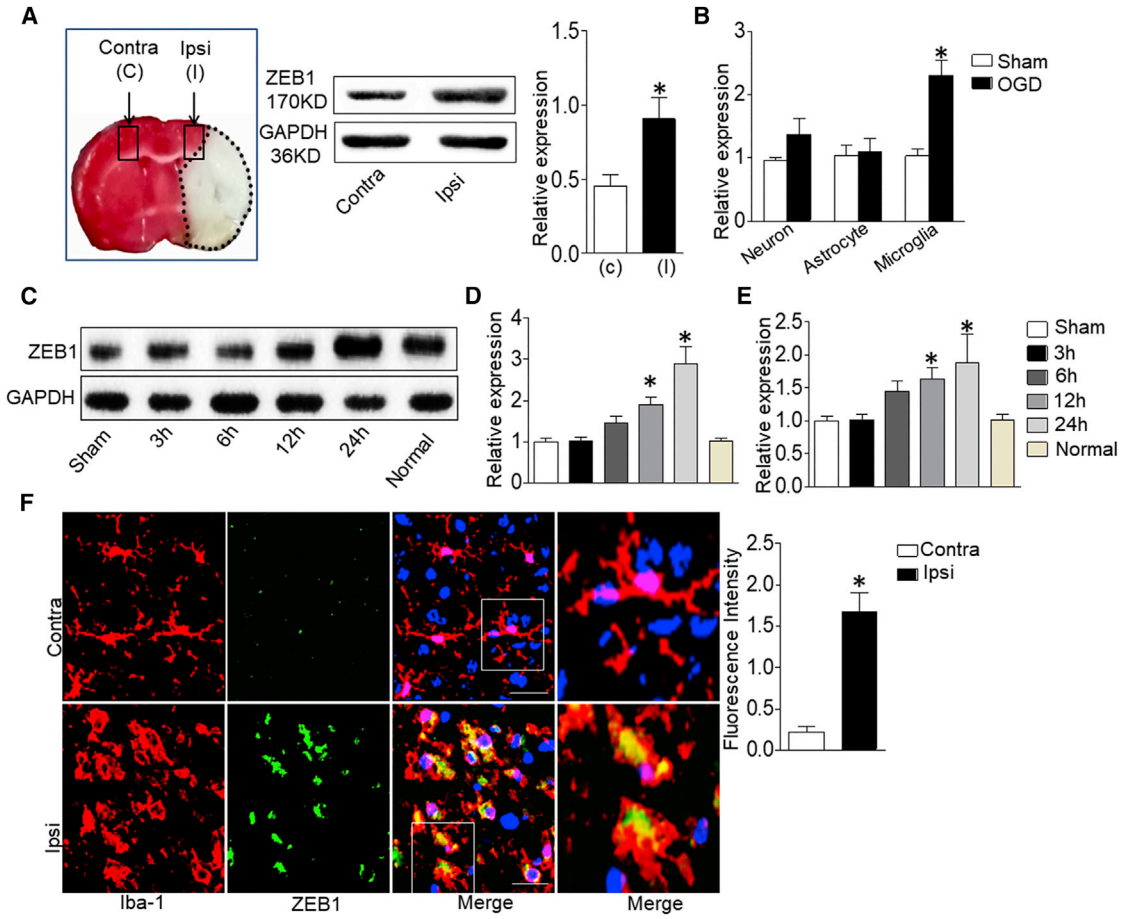

Figure 1. ZEB1 Expression Is Dramatically Elevated in Microglia after Stroke

(A) ZEB1 protein levels were examined from the contralateral cortex (C) and ischemic ipsilateral cortex (I) of mice that underwent tMCAO after 24 hr of reperfusion. Western blots were analyzed with ImageJ software and normalized to GAPDH expression. Left panel shows representative TTC staining of brain sections from tMCAO mice.

(B) ZEB1 transcription level in primary neurons, astrocytes, and microglia after OGD for 24 hr.

(C) ZEB1 expression in primary microglia undergoing OGD for 0, 3, 6, 12, or 24 hr followed by exposure to a normal oxygen concentration level for 24 hr.

(D) Quantitation and statistical evaluation of data in (C). Ordered bars correspond to ordered lanes in (C).

(E) qPCR analysis of ZEB1 expression after OGD for 0, 3, 6, 12, or 24 hr and after normal oxygen concentration for 24 hr.

(F) Representative immunohistochemical staining for microglia and ZEB1 from contralateral (Contra) and ipsilateral (Ipsi) regions of ischemic penumbra of brain tissue after tMCAO. Rightmost panel shows inset box to left at a higher magnification. Intensity of ZEB1 immunofluorescence was quantified using ImageJ. Scale bars, 20 μm.

Data indicate means ± SEM (n = 6 per group). *p < 0.05.

inflammatory milieu after ischemic stroke. We propose that ZEB1 is a key regulator of microglia responses in the events after ischemic stroke and may be critically involved in neuroinflammation.

RESULTS

Microglial ZEB1 Is Upregulated after Acute Brain Ischemia

To examine the specific molecular mechanisms of inflammation in the ischemic brain, we explored possible molecular factors that might contribute to the inflammatory response soon after ischemic stroke. We developed a mouse model of ischemic stroke by adapting the Longa method (Li et al., 2016). 24 hr after the induction of transient middle cerebral artery occlusion (tMCAO), we removed cortical samples from the contralateral side and the penumbra of the mouse brains and then examined ZEB1 expression using western blot. As Figure 1A depicts, ZEB1 expression was higher in the ischemic hemisphere compared the contralateral hemisphere.

Next, to examine which cell type exhibited ZEB1 upregulation after tMCAO, we isolated and cultured microglia, astrocytes, and neurons from brains of neonatal mice (Dagda and Rice, 2017; Li et al., 2016). We then subjected these cells to oxygen-glucose deprivation (OGD; 1% oxygen and 99% nitrogen). qPCR analysis showed that, although microglia and neurons exhibited elevated ZEB1 expression, microglia displayed greater ZEB1 expression (Figure 1B). In primary microglia subjected to OGD at several

time points, we found that ZEB1 expression progressively increased with longer periods of OGD, and then ZEB1 mRNA and protein levels returned to baseline levels after exposure to normal oxygen concentrations for 24 hr (Figures 1C–1E). Immunohistochemical staining of brain sections corroborated the qPCR results, showing that ZEB1 staining in microglia was more intense and concentrated in the ipsilateral hemisphere compared to the contralateral hemisphere (Figure 1F). These data suggest that ZEB1 expression is upregulated in the ischemic penumbra and that activated microglia are the main source of ZEB1 there.

Characterization of *ZEB1*-Knockdown and *ZEB1*-Transgenic Mice

To investigate the involvement of microglial ZEB1 in ischemic stroke, we examined mice that expressed lower levels of microglial ZEB1 (knockdown [KD]; *ZEB1*-KD) and mice that overexpressed microglial ZEB1 (transgenic [TG]; *ZEB1*-TG). First, we generated *Zeb1*-TG mice and *Zeb1*-KD mice, which harbor, respectively, a stop element of the *Zeb1* gene flanked by a *loxP* site or exon 4 of the *Zeb1* gene flanked by a *loxP* site (Figure 2A). Mice carrying *loxP*-flanked *Zeb1* alleles were crossed with mice expressing *CX3CR1*^{CreER} (Figure 2B). *ZEB1*-TG mice were generated by crossing *CX3CR1*^{CreER} mice and *Zeb1*-TG mice, and *ZEB1*-KD mice were generated by crossing *CX3CR1*^{CreER} mice and *Zeb1*-KD mice.

We first assessed microglial ZEB1 expression in *ZEB1*-KD mice and found that both ZEB1 mRNA and protein levels were downregulated. ZEB1 expression in splenic monocytes, however, was not downregulated. Unlike in *ZEB1*-KD mice, microglial ZEB1 expression in *ZEB1*-TG mice was upregulated compared to their wild-type (WT) littermates (Figures 2C and 2D). *ZEB1*-KD and *ZEB1*-TG mice developed normally, showing no obvious signs of neurological disease, infertility, or behavioral abnormalities. There were also no differences in either gross brain structure or the number of astrocytes, microglia, and neurons (Figures S1A–S1C). Flow-cytometric analysis showed that differential expression of microglial ZEB1 did not affect the number of peripheral immune cell subtypes (Figures S1D and S1E).

Targeted Overexpression of Microglial ZEB1 Reduces Acute Ischemic Brain Injury

After induction of tMCAO, we first tested the neurological function of WT, *ZEB1*-TG, and *ZEB1*-KD mice. *ZEB1*-KD mice had more severe neurological deficits than WT mice, and *ZEB1*-TG mice were less impaired in the components of the modified Neurological Severity Score (mNSS), foot-fault test, and corner-turning test (Figures 2E, 2G, and 2H) after tMCAO. Performance in the adhesive-removal test was statistically indistinguishable across the three groups of mice (Figure 2F). Analysis of 2,3,5-triphenyltetrazolium chloride (TTC) staining (Figure 2I) supported the behavioral results. After reperfusion, *ZEB1*-KD mice had significantly larger infarcts than WT mice, whereas *ZEB1*-TG mice had smaller infarcts. The protective impact of microglial ZEB1 on brain injury may persist through the acute stage to late stages of stroke (Figure S2). Examination of blood-brain barrier (BBB) permeability revealed that the *ZEB1*-TG mice had significantly less Evans blue extravasation compared to WT mice, and as expected, *ZEB1*-KD mice had significantly more extravasation (Figure 2J, right panel). Since cell apoptosis is a well-known hallmark following stroke, we used a propidium iodide (PI)-annexin V kit to test for apoptotic cells after tMCAO. In *ZEB1*-TG mice, fewer cells in the ischemic hemisphere underwent apoptosis, but in *ZEB1*-KD mice, more cells underwent apoptosis than in WT mice (Figure 2K). Also, reactive oxygen species in the *ZEB1*-TG group were reduced compared to those in the WT group (Figure S3). Taken together, these results indicate that selective overexpression of microglial ZEB1 plays a protective role after ischemic stroke.

ZEB1 Affects Microglia Morphology and Activity after tMCAO

Since microglia are key immune cells that can respond quickly to environmental changes in the brain, we focused specifically on microglia and investigated ZEB1-mediated microglia response. First, we performed detailed quantitative morphometric analysis of Iba-1-positive microglia in the hippocampus, neocortex, and cerebellum of transgenic mice and WT mice under normal conditions. As demonstrated in three-dimensional reconstructions of confocal z stacks of imaged Iba-1-positive microglia, *ZEB1*-KD microglia showed fewer sparsely spaced processes compared to microglia from WT mice, and *ZEB1*-TG microglia showed a distinct arborization pattern of finely delineated processes (Figure 3A, schematic). Corroborating this observation, Sholl analysis revealed that the processes of *ZEB1*-TG microglia were more complex than those of WT microglia and that the processes of *ZEB1*-KD microglia were less complex (Figure 3A, graph on right).

We next counted the numbers of Iba-1-positive microglia in WT, *ZEB1*-TG, and *ZEB1*-KD mice after tMCAO. While we found no difference across the three groups in the penumbra region (Figures 3B and 3C). The summed lengths of microglial processes and the percentages of ameboid microglia across the three groups were similar (Figures 3D and 3E). We also assessed the degree of activation of microglia by quantifying microglia shapes using image analysis of 2D somatic projections. Shape parameters were calculated based on measuring maximum length (L) and projection area (A) of individual imaged microglia. When microglia became activated, the somatic shape index (L/A) decreased. However, the L/A ratio in WT mice was larger than in *ZEB1*-TG mice and smaller than in *ZEB1*-KD mice (Figures 3F and 3G).

Lastly, we assessed the apoptosis and proliferation rate of microglia using a (PI)-annexin V kit and Ki-67. In this experiment, microglia was referred to as CD11b^{+}CD45^{low}. Examination of the extent of microglial apoptosis and proliferation revealed no differences between WT, *ZEB1*-TG, and *ZEB1*-KD mice (Figures 3H and 3I). Overall, these data indicate that, after ischemic stroke, ZEB1 is associated with microglia having a more ramified morphology and a less reactive phenotype.

ZEB1 Expression Is Associated with a Distinctive Microglial Gene Expression Profile

To further investigate whether ZEB1 affects microglia function after ischemic stroke, we performed mRNA microarray (Agilent

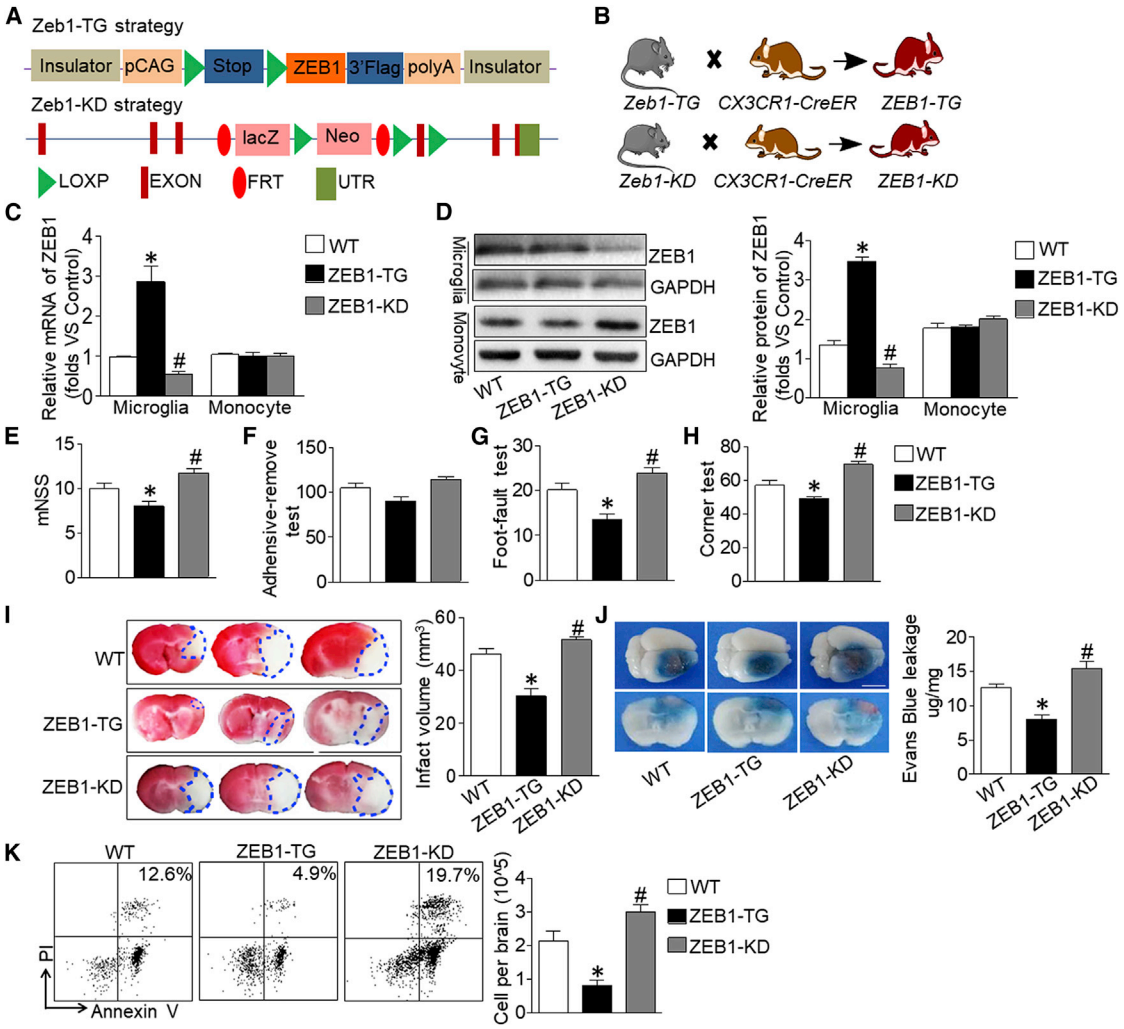

Figure 2. Microglia-Specific ZEB1 Upregulation Reduces Neurovascular Injury after Ischemia

(A) Gene strategy for preparing *Zeb1*-TG and *Zeb1*-KD mice.

(B) Breeding scheme for *CX3CR1*$^{Cre\ ER}$ mice crossed with *Zeb1*-TG or *Zeb1*-KD mice. The offspring for the former are denoted as *ZEB1*-TG, in which ZEB1 is overexpressed in microglia; the latter are denoted as *ZEB1*-KD mice, in which ZEB1 is downregulated in microglia.

(C) Relative expression of ZEB1 mRNA in microglia and splenic monocytes from *ZEB1*-TG, *ZEB1*-KD mice, and wild-type (WT) mice, assessed using qPCR.

(D) ZEB1 expression was detected in microglia and monocytes by western blot.

(E–H) 24 hr after tMCAO, we evaluated neurological deficits of in WT, *ZEB1*-TG, and *ZEB1*-KD mice after tMCAO using the mNSS (E), adhesive-removal test (F), foot-fault test (G), and corner-turning test (H) in WT, ZEB1-TG, and ZEB1-KD mice.

(I) TTC staining was used to evaluate infarct volumes in the three groups 24 hr after tMCAO. After staining, undamaged tissue appears deep red, and infarcted tissue remains white. Dashed lines encompass the estimate of infarct at one rostro-caudal level. Infarct volumes were quantified using Image-Pro-Plus v.5.0 software (right panel).

(J) Evans blue extravasation in WT, *ZEB1*-TG, and *ZEB1*-KD mice. Top row: dorsal view of whole brain; bottom row: representative rostro-caudal levels of Evans-blue-stained tissue.

(K) 24 hr after tMCAO, the number of apoptotic cells from brains of the three groups were assessed using an annexin-PI kit and fluorescence-activated cell sorting (FACS).

*p < 0.05 (*ZEB1*-TG versus WT); #p < 0.05 (*ZEB1*-KD versus WT). Data indicate mean ± SEM (n = 6 per group). See also Figures S1, S2, and S3.

Technologies) analyses, which generated microglia-specific gene expression profiles. ZEB1 affected the expression not of single genes or small gene clusters but thousands of genes, leading to what appears to be a "complete reprogramming" of microglia. Microarray gene profiles clearly distinguished microglia from WT, *ZEB1*-TG, and *ZEB1*-KD mice (Figure 4A). Using a more than 2-fold change threshold, we observed that ZEB1 significantly influences gene expression in microglia.

Next, we performed a Gene Ontology analysis of the differentially expressed genes from all comparisons, using the Database for Annotation, Visualization, and Integrated Discovery (DAVID) to gain an overview about the nature of gene and potential shared

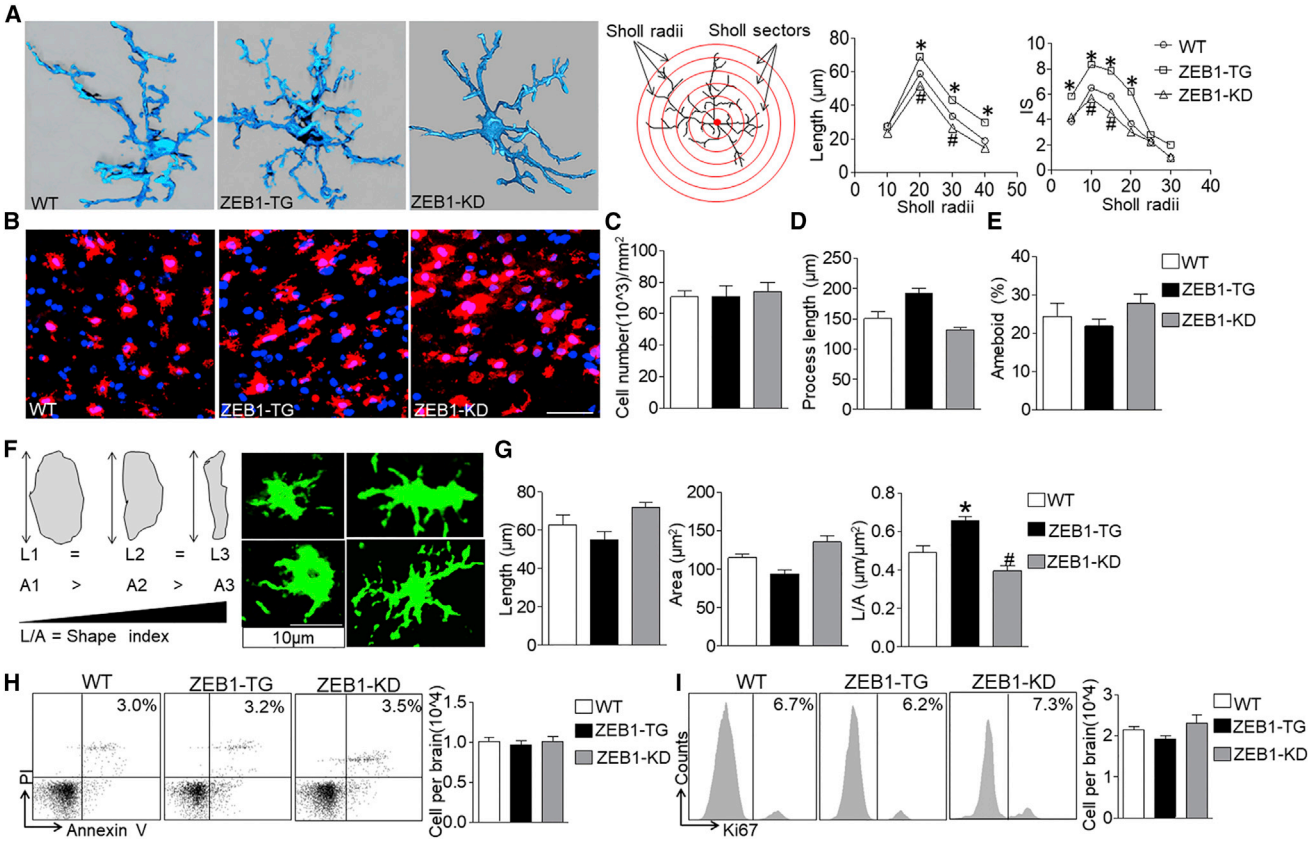

Figure 3. Effects of ZEB1 Expression on Microglial Morphology

Morphological correlates of microglia activation assessed with an antibody against anti-Iba-1, a microglial marker.

(A) Detailed morphology of microglia in WT mice under normal conditions. The three left panels show Imaris (Bitplane)-based three-dimensional reconstructions of representative microglia in WT, *ZEB1*-TG, and *ZEB1*-KD mice. Middle: schematic diagram of a three-dimensional Sholl grid of concentric spheres centered on the geometric center of the microglia cell somata (red cross). Branch crossings along the spherical grid allowed us to quantify the number and branch lengths of three-dimensionally reconstructed microglial processes between consecutive spheres. This provides an estimate of the degree of microglial process complexity. The graphs on the right show the Sholl quantitation of microglial processes. IS, segment interactions.

(B) Representative confocal images of immunohistochemical staining of microglia in the penumbra of WT, *ZEB1*-TG, and *ZEB1*-KD mice. Scale bar, 50 μm.

(C) Iba-1-positive cells were counted in the penumbra of immunohistochemically stained brain sections from WT, *ZEB1*-TG, and *ZEB1*-KD mice.

(D) Total process lengths of confocal images of immunostained microglia were analyzed by Image J.

(E) Percentage of ameboid microglia in the penumbra of WT, *ZEB1*-TG, and *ZEB1*-KD mice.

(F) Shape analyses of two-dimensional somatic projections based on maximum length (L) and projection area (A) in confocal images of Iba-1-immunostained microglia (right) using ImageJ. The somatic shape index (L/A ratio) increases in rod-shaped somata.

(G) Quantitation of microglial somata L, A, and the L/A ratio.

(H) Apoptosis flow-cytometric analyses of microglia after tMCAO.

(I) Proliferation of microglia in WT, *ZEB1*-TG, and *ZEB1*-KD mice after tMCAO, as revealed by FACS analysis of Ki-67-stained cells.

*$p < 0.05$ (*ZEB1*-TG versus WT); #$p < 0.05$ (*ZEB1*-KD versus WT). Data indicate means ± SEM. n = 6 per group.

pathways (Huang et al., 2009). Here, we listed the top 10 enriched clusters in the comparison of WT/*ZEB1*-TG (Figure 4B) with WT/*ZEB1*-KD (Figure 4C). Interestingly, several of these enriched terms were shared between the different pairwise comparisons including immune system process, innate immune response, and cellular response to interferon (IFN)-β which are involved in inflammation and cell response. Under normal (non-tMCAO) conditions, these Gene Ontology terms were not involved in the comparison of WT/*ZEB1*-TG with WT/*ZEB1*-KD (Figure S4). Therefore, ZEB1 is very important for microglia plasticity. Microglial ZEB1 may play a role in monitoring the local environment and regulating the immune response after ischemic stroke.

Neutrophil Infiltration Is Attenuated with Microglial ZEB1 Overexpression

To determine the potential impact of microglia ZEB1 on the immune response after tMCAO, we measured the accumulation of leukocytes in the brains of WT, *ZEB1*-TG, and *ZEB1*-KD mice after tMCAO by using flow cytometry. The gating strategy is shown in Figure 5A. 24 hr post-tMCAO reperfusion, we found no difference between WT, *ZEB1*-TG, and *ZEB1*-KD mice in the numbers of microglia, $CD4^+$T cells, $CD8^+$ T cells, natural killer (NK) cells, B cells, or macrophages; Similarly, CD86-positive and CD206-postive microglia counts did not differ (Figure 5B). In contrast, *ZEB1*-TG mice had decreased

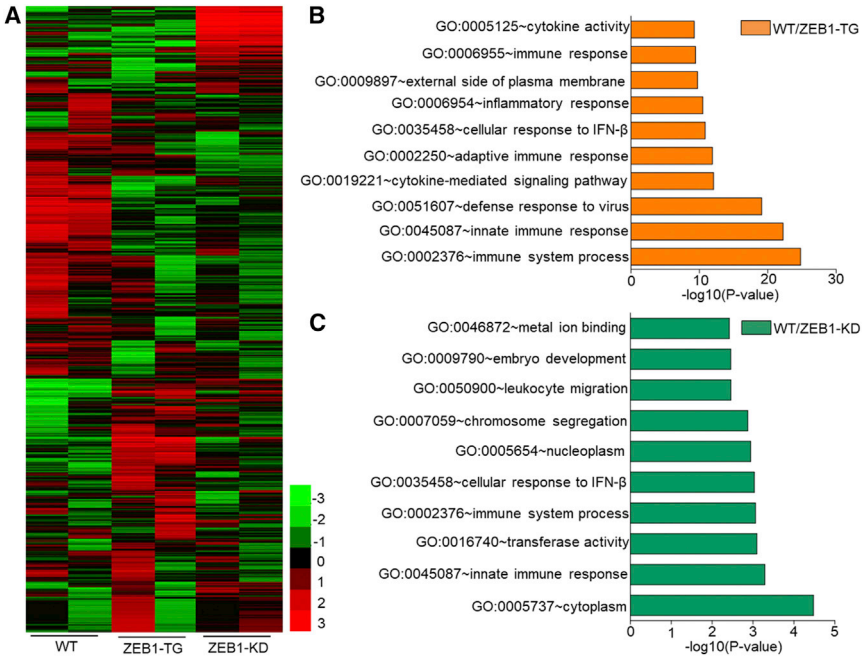

Figure 4. Effect of ZEB1 Expression on the Molecular Profiles of Microglia

Microglia were isolated from the brains of WT, *ZEB1*-TG, and *ZEB1*-KD mice by using a CX3CR1 selection kit.

(A) Heatmap of gene profiles of microglia in WT, *ZEB1*-TG, and *ZEB1*-KD mice.

(B) The ten most enriched clusters in the comparisons of WT and *ZEB1*-TG mice, including the $-\log_{10}$ (P value), are shown.

(C) The 10 most enriched clusters in the comparisons of WT and *ZEB1*-KD mice, including the $-\log_{10}$ (P value), are shown. (n = 2 per group).

See also Figure S4.

accumulations of neutrophils in the brain, while *ZEB1*-KD mice had increased neutrophil infiltration compared with WT mice (Figures 5B and 5D). These significant differences persisted up to 3 days after tMCAO (Figure 5E). Interestingly, the spleens of *ZEB1*-TG mice exhibited increased numbers of neutrophils but no increase of any other leukocyte subtype. The spleens of *ZEB1*-KD and WT mice had comparable numbers of neutrophils (Figures 5C and 5F). We also analyzed monocytes after tMCAO, since monocytes infiltrate the brain in large quantities during acute ischemic stroke (Kriz and Lalancette-Hébert, 2009). The number and phenotype of monocytes in the three groups did not differ (Figure S5). When depleting neutrophils in *ZEB1*-TG and *ZEB1*-KD mice, the clinical score and infarct volumes were similar to those of WT mice (Figure S6). These results suggest that overexpression of microglial ZEB1 may lead to a reduction in the accumulation of neutrophils in the ischemic brain.

ZEB1 Enhancement Decreases Neutrophil Chemoattractant C-X-C Motif Ligand 1

We showed that neutrophils rapidly infiltrate the CNS after tMCAO, contributing to inflammation and aggravating brain damage. This selective migration of neutrophils depends on many molecules and chemokines that emerge after ischemic stroke (Murikinati et al., 2010). We first examined neutrophil-attracting chemokines and found that mRNA levels of C-X-C motif ligand 1 (CXCL1)—a chemokine that mainly recruits neutrophils—dramatically decline only in the *ZEB1*-TG mice after tMCAO (Figure 6A). Given that astrocytes and microglia are the first cells that respond in ischemic stroke, we reasoned that one of these might be the major source of brain CXCL1. Double-immunofluorescent staining of brain sections from WT mice with anti-Iba-1 and anti-CXCL1 (for microglia), anti-glial fibrillary acidic protein (GFAP) and anti-CXCL1 (for astrocytes), and anti-NeuN and anti-CXCL1 (for neurons) indicated that astrocytes are the source of brain CXCL1 after tMCAO (Figure 6B). In *ZEB1*-TG mice, CXCL1-GFAP double-immunofluorescent staining showed, as expected, that CXCL1 staining intensity was reduced compared to that in WT mice (Figure 6C, D). These results suggest that microglia-derived ZEB1 can affect the expression of CXCL1 in the ischemic brain.

Transmigration of Spatially Isolated Neutrophils Is Reduced in Astrocyte-Microglia Co-cultures from *ZEB1*-TG Mice

Since astrocytes are the major source of CXCL1, we investigated whether astrocytes from WT mice and *ZEB1*-TG mice differed in their ability to induce neutrophil migration. Using purified astrocytes from WT and *ZEB1*-TG mice, we exposed them to OGD for 12 hr and then cultured them for 4 hr in a Transwell system with purified neutrophils separated by a Transwell membrane (neutrophils in the upper chamber) (Figure 7A); the purity of cells is shown in Figure S7. The proportions of neutrophils that had migrated into the lower Transwell chamber were not significantly different between cultures of WT and *ZEB1*-TG astrocytes (Figure 7B, left). ELISA analysis for CXCL1 in the supernatants of cultured astrocytes also failed to detect a difference in the concentration of CXCL1 between the two groups (Figure 7B, right). Thus, we hypothesized that microglia may play a role in the migration of these neutrophils *in situ*.

Microglia and astrocytes from WT and *ZEB1*-TG mice were co-cultured, and again, using the same Transwell system, we calculated a neutrophil migration index. After 12 hr, the migration of neutrophils from *ZEB1*-TG mice in the mixed-glial cultures was dramatically reduced compared to neutrophils from WT mixed-glial cell cultures (Figure 7C, left); ELISA analysis also showed significantly reduced CXCL1 in the supernatant of *ZEB1*-TG mixed-glial cell cultures (Figure 7C, right).

To assess whether cytokines produced by microglia might influence CXCL1 content in astrocytes, we used a conditioned medium system, immunofluorescent staining, and flow cytometry (Figure 7D). After 12 hr, we measured astrocyte-secreted CXCL1

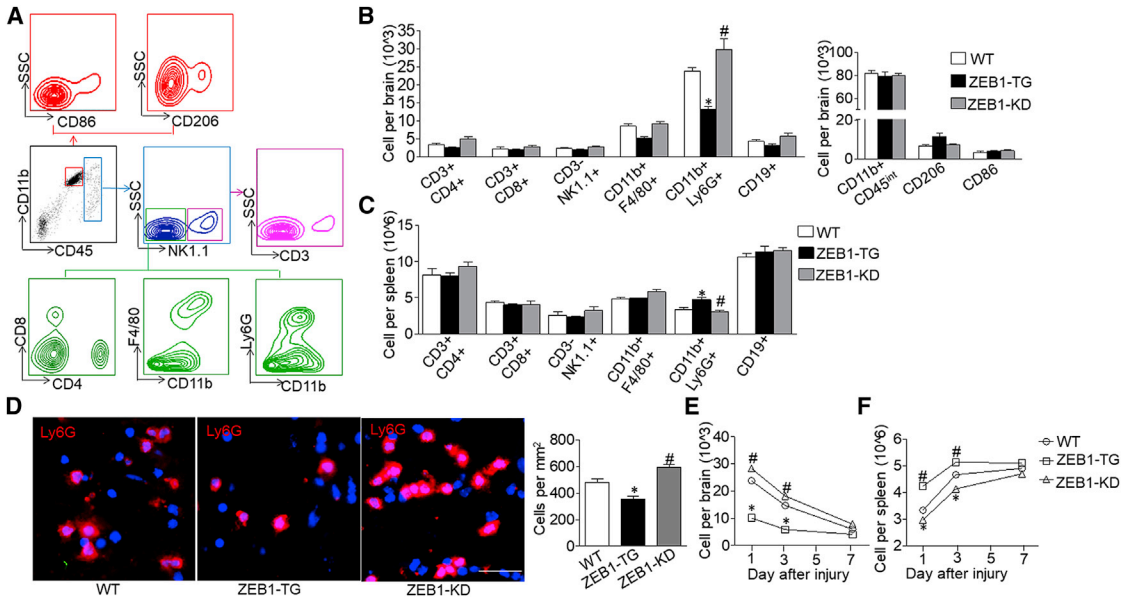

Figure 5. Neutrophil Infiltration Is Attenuated with Microglial ZEB1 Overexpression

(A) Gating strategy for leukocytes and subtypes and microglia isolated from the brain after tMCAO. Fluorescence minus one (FMO) controls were used in the gating strategy.

(B) Counts of macrophages, neutrophils, $CD4^+$ T cells, $CD8^+$ T cells, NK cells, B cells and microglia, and CD86-expressing and CD206-expressing microglia in brains of WT, *ZEB1*-TG, and *ZEB1*-KD mice 24 hr after tMCAO. Data represent absolute cell numbers per brain.

(C) Counts of splenocytes in WT, *ZEB1*-TG, and *ZEB1*-KD mice 24 hr after tMCAO.

(D) Immunofluorescent staining of brain sections shows representative density of neutrophils in peri-infarct areas of WT, *ZEB1*-TG, and *ZEB1*-KD mice 24 hr after tMCAO. Scale bar, 20 μm.

(E and F) Neutrophils were quantified by using flow cytometry of brain (E) and spleen (F) cells of WT, *ZEB1*-TG, and *ZEB1*-KD mice 1, 3, and 7 days after tMCAO. Data indicate means ± SEM. n = 6 per group. *$p < 0.05$ WT versus *ZEB1*-TG mice; #$p < 0.05$ WT versus *ZEB1*-KD mice. See also Figures S5 and S6.

in conditioned medium from WT or *ZEB1*-TG cultures (Figure 7E) and observed that the fluorescence intensity and percentage of CXCL1 were significantly reduced in astrocytes from *ZEB1*-TG microglia-conditioned medium. Thus, microglia appear to engage in "crosstalk" with astrocytes, inhibiting the production of CXCL1 by astrocytes. In addition, microglial ZEB1 overexpression shows a more potent inhibitory effect during the process.

We next used qPCR and the neutrophil Transwell system to investigate which microglial cytokine influences CXCL1 production in astrocytes. Since WT and *ZEB1*-TG microglia differed in their content of several cytokines, we sequentially applied antibodies of tumor necrosis factor α (TNF-α), interleukin (IL)-4, IL-6, or transforming growth factor β1 (TGF-β1) to block the action of each cytokine in the Transwell experiment (Figure 7F). Only by blocking TGF-β1 did the neutrophil migration indexes in the WT and *ZEB1*-TG groups become equal (Figure 7G). Presumably, then, in *ZEB1*-TG mice, microglia can inhibit astrocytic CXCL1 production by secreting TGF-β1. Astrocytes cultured with *ZEB1*-TG microglia-conditioned medium produced more p-SMAD2/3, as assessed by both western blot and flow-cytometric analyses (Figure S8), further substantiating the hypothesis that microglia can communicate with astrocytes through the TGF-β1 pathway and inhibit the latter's production of CXCL1; ZEB1 overexpression facilitates this.

To investigate the mechanism of how ZEB1 regulates TGF-β1 in microglia, we conducted a series of experiments in a microglia cell line, BV2 cells. First, BV2 cells were transfected with the ZEB1 expression or control plasmid, and the mRNA of TGF-β1 was tested by qPCR. The mRNA was increased after the transfection of ZEB1 expression plasmid (Figure 7H). Then, we performed the luciferase assays to elucidate the molecular mechanism by which ZEB1 regulates TGF-β1 transcription. As shown in (Figure 7I), the luciferase assay indicated that ZEB1 overexpression increases the promoter activity of the TGF-β1-p-1.8k reporter up to 3-fold, relative to control BV2 cells. Next, we conducted chromatin immunoprecipitation (ChIP) assays to detect whether ZEB1 could directly bind to the E_2-box. The assays revealed that ZEB1 could bind to the TGF-β1 promoter under basal conditions in an E_2-box-dependent manner. Importantly, quantitative ChIP assays indicated that ZEB1 overexpression results in an increase in its binding to the area of E_2-box1, E_2-box2. However, the recruitment of ZEB1 to E_2-box3 was less evident (Figure 7J). These observations indicate that ZEB1 binds directly to the endogenous TGF-β1 promoter at the positions −643/−637 and −917/−911, resulting in the transcriptional activation of TGF-β1.

Blockade of TGF-BRII in Astrocytes Abolishes the Protective Effect in *ZEB1*-TG Mice

Microglial TGF-β1 production was measured 1, 3, and 7 days after tMCAO and reperfusion. In *ZEB1*-TG mice, microglial TGF-β1 production was greater than WT mice (Figures 8A and 8B), especially

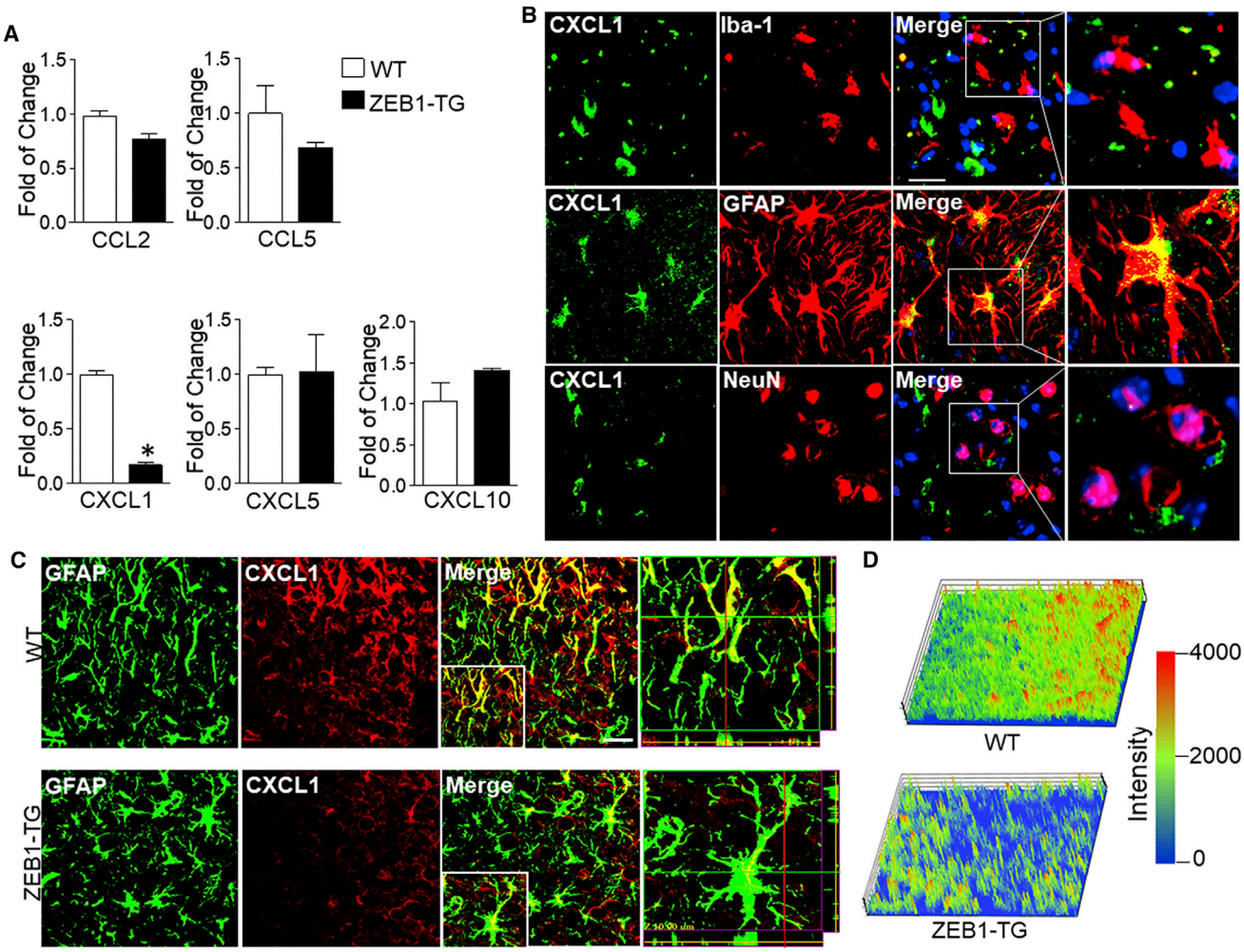

Figure 6. Microglia-Targeted ZEB1 Expression Reduces Neutrophil Chemoattractant CXCL1 Derived from Astrocytes

(A) qPCR analysis of chemokines related to the infiltrated neutrophils in WT and *ZEB1*-TG mice after tMCAO.

(B) Confocal microscopy images of WT brain sections double-immunofluorescent stained for Iba-1 and CXCL1, for GFAP and CXCL1, and for NeuN and CXCL1. Scale bar, 10 μm.

(C) Similar immunohistochemical experiments with WT and *ZEB1*-TG mice, showing robust spatial overlap of GFAP and CXCL1 immunostaining after tMCAO. Boxes in the third column of panels are shown in higher magnification in the adjacent panels. Reference boxes in the rightmost panels indicate area over which 2.5 dimensional (2.5D) staining intensity analysis of CXCL1 was done. Scale bar, 50 μm.

(D) Results of a 2.5D intensity analysis of CXCL1 immunostaining. Data are means ± SEM. *$p < 0.05$.

1 day after tMCAO (Figures 8C and 8D). To determine whether microglia of *ZEB1*-TG mice secrete more TGF-β1 and influence CXCL1 content in astrocytes, we manufactured an adeno-associated virus (AAV) harboring a GFAP promoter and encoding region for TGF-BRII, a TGF receptor (Figure 8E). AAV-shTGFBRII (6×10^9 IU) or control AAV was injected into the brains of WT mice. Three weeks after transfection, the mice underwent tMCAO. Twenty-four hours later, their brains were removed, and cells were analyzed by flow-cytometric analysis. Histogram plots showed that the number of TGF-BRII receptors in astrocytes were dramatically smaller in the AAV-shTGFBRII-transfected mice compared with those in AAV-control mice (Figure 8F).

We next examined the number of neutrophils in the brains and spleens of WT and *ZEB1*-TG mice injected with AAV-shTGFBRII or AAV-control after tMCAO. After tMCAO, although neutrophil infiltration into the brains of AAV-shTGFBRII-transfected *ZEB1*-TG mice equaled that in AAV-control-transfected WT mice, neutrophil infiltration into the brains of AAV-control-transfected *ZEB1*-TG mice was markedly reduced. AAV-shTGFBRII-transfected mice showed no difference in the number of neutrophils, but AAV-control-transfected *ZEB1*-TG mice had greater neutrophil counts in the spleen compared to AAV-control-transfected WT mice (Figure 8G).

Confocal microscopy of immunofluorescent staining of astrocytes showed that astrocytes from AAV-shTGFBRII-transfected WT and *ZEB1*-TG mice did not differ significantly in CXCL1 content. By contrast, astrocytes from

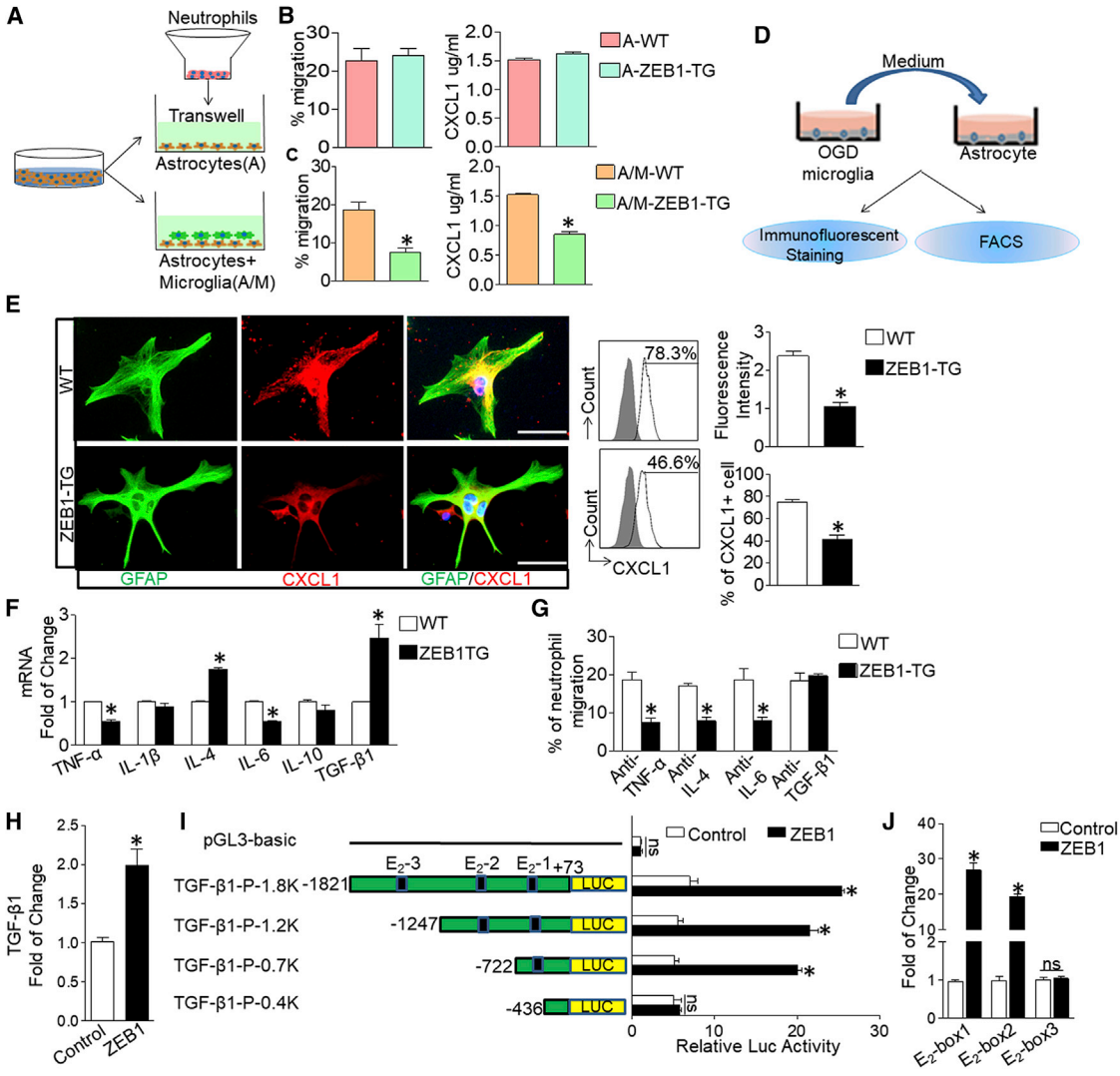

Figure 7. Reduced Transmigration of Neutrophils in Astrocyte-Microglial Co-cultures from *ZEB1*-TG Mice

(A) General schematic of the Transwell system, with primary astrocytes alone or co-cultured with microglia.

(B) After astrocytes were isolated from WT and *ZEB1*-TG mice and exposed to OGD, neutrophil migration was measured by flow cytometry (FCM). CXCL1 in the supernatant of astrocytes was also analyzed by ELISA.

(C) Microglia and astrocytes were co-cultured in the lower chamber of the Transwell system and exposed to OGD. Migration of neutrophils and CXCL1 in the supernatant was measured by flow cytometry and ELISA, respectively.

(D) Procedure for the conditioned medium system of microglia and astrocytes. Microglia from both WT and *ZEB1*-TG mice were harvested and cultured for 12 hr under OGD conditions. Conditioned medium was collected and added to the astrocytes for the next 12 hr. Expression of CXCL1 in astrocytes was measured by flow cytometry and immunofluorescent staining.

(E) Expression of CXCL1 in astrocytes was examined by immunofluorescent staining and flow cytometry. Scale bars, 20 μm.

(F) Main cytokines produced by microglia that might affect CXCL1 expression were measured by qPCR.

(G) Antibodies against TNF-α, IL-4, IL-6, and TGF-β1 were added to the conditioned medium, and the migration of neutrophils was measured in the Transwell system.

(H) The mRNA of TGF-β1 after transfected with the ZEB1 expression or control plasmid.

(I) BV2 cells were co-transfected with the ZEB1 expression plasmid and different wild-type or truncated TGF-β1 promoter luciferase reporter constructs. Cell-extract luciferase activities were determined 36 hr after transfection using a Betascope analyzer. Luciferase values were normalized to Renilla activities.

(J) Association of ZEB1 with the TGF-β1 promoter was analyzed by a quantitative ChiP assay.

Data indicate means ± SEM. *p < 0.05. See also Figures S7 and S8.

AAV-control-transfected *ZEB1*-TG mice showed significantly less CXCL1 (Figure 8H). This suggests that microglial ZEB1 suppressed astrocytic CXCL1 secretion via the TGF-β1 signaling pathway.

DISCUSSION

Because of the growing global incidence of ischemic stroke, there is a compelling need to discover new ways to mitigate

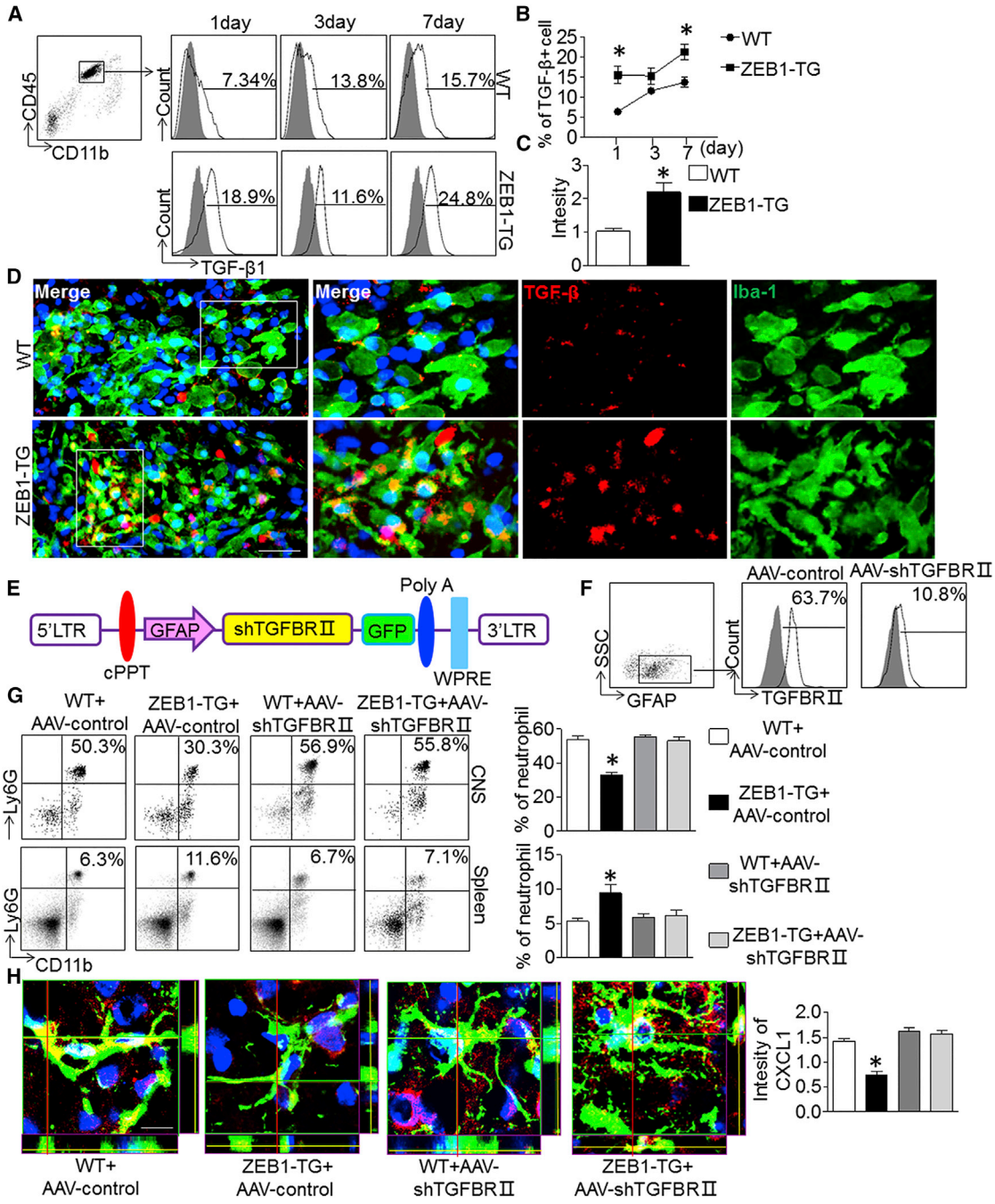

Figure 8. Blocking TGF-BRII in Astrocytes Abolishes the Protective Effect of ZEB1 Overexpression in *ZEB1*-TG Mice

(A) Microglial TGF-β1 expression was tested by flow cytometry 1, 3, and 7 days after tMCAO and reperfusion in WT and *ZEB1*-TG mice.

(B) Statistical analysis of TGF-β1 expression.

(C and D) 24 hr after reperfusion, TGF-β1 and Iba-1 double-immunofluorescent staining was evaluated in brain sections from the penumbra of ischemic mice (D); the graph shows relative intensities of TGF-β1 expression (C). Scale bar, 50 μm.

(E) Schematic map of the astrocyte-specific AAV-shTGFBRII.

(F) 24 hr after tMCAO, cells from the brain tissues underwent flow cytometry analysis. Histograms and quantification show expression of TGF-BRII in astrocytes from AAV-shTGFBRII- or control AAV-transfected mice 24 hr after tMCAO.

(G) 24 hr after reperfusion, the number of neutrophils in the brains and spleens of WT and *ZEB1*-TG mice was measured by flow cytometry.

(H) Confocal microscopy images of anti-CXCL1/anti-GFAP double-immunostained astrocytes were used to measure astrocytic CXCL1 content (green indicates GFAP; red indicates CXCL1, blue indicates nuclei stained with DAPI). Scalebar: 20 μm.

Data indicate means ± SEM; n = 6 per group. *p < 0.05.

the disabling consequences of stroke. The immune system has been consistently implicated in the pathophysiology of stroke aftermath, and its activation is associated with unfavorable outcomes. In this study, we explored the contribution of a transcription factor, ZEB1, as a key molecular factor in regulating post-stroke inflammatory events.

After ischemic insult to the CNS, excitotoxicity, calcium dysregulation, oxidative and nitrosative stress, and inflammation are the most prominent processes leading to cell and tissue damage in the ischemic tissue (Moskowitz et al., 2010). The potentially salvageable tissue around the core of the ischemic tissue, referred to as the penumbra, is a prime region to target. Our experiments demonstrated that ZEB1 expression is elevated in the penumbra under ischemic conditions, and elevated ZEB1 expression specifically localizes to microglia. The present experiments used conditional transgenic mice to determine whether ZEB1 specifically expressed in microglia is involved in the pathological immune responses after ischemic stroke and, if so, to determine what physiological role ZEB1 plays in post-ischemic responses.

To overcome the lack of specific tools to delineate the function of microglia in pathophysiological processes, we used a genetic tool that specifically and inducibly manipulated microglia by invoking the expression of Cre recombinase driven by the *CX3CR1* promoter coupled with estrogen receptor. This technique takes advantage of microglia's longevity and concomitant self-renewal (Parkhurst et al., 2013; Wieghofer et al., 2015). Although myeloid cells and microglia express CX3CR1 (White and Greaves, 2012; Yona et al., 2013), there are many differences between these two cell types. Microglia are a self-renewing population with a low turnover rate (Ajami et al., 2007), while myeloid cells (e.g., monocytes, dendritic cells, NK cells, and T cells) will replenish with CX3CR1^{-} bone marrow precursor with a rapid turnover rate (Zhang et al., 2014; Arnold et al., 2012). Based on these differences, we used *CX3CR1*^{CreER} mice to achieve selective genetic modification of microglia. Four weeks after tamoxifen administration, Cre-dependent modification of the gene was almost exclusively in microglia (Parkhurst et al., 2013). In *ZEB1*-KD microglia, ZEB1 expression was downregulated by approximately 50%. In *ZEB1*-KD mice, the *loxP* site is located on one of the alleles. When *loxP* mice were crossed with *CX3CR1*^{CreER} mice, only one allele of *zeb1* exon is cut away, and another allele could still express *zeb1* (heterozygous). Thus, ZEB1 expression still occurred. *ZEB1*-TG mice subjected to tMCAO had less severe brain injuries than their WT controls. In a previous study of ischemic stroke, ZEB1 induction provided a protective response, since neurons from ZEB1$^{-/-}$ animals proved to be the more vulnerable to OGD (Bui et al., 2009). This indicated that ZEB1 is a protective molecule that is expressed after ischemic stroke.

Microglia are so-called "housekeepers" of the brain, constantly "surveying" the local microenvironment, maintaining brain homeostasis, and responding to injury by extending or retracting their filopodia-like protrusions (Benarroch, 2013; Nimmerjahn et al., 2005). The ramified shape of microglia determines its function. Our morphological analyses showed that there are more ramified microglia with more complex processes and branches in *ZEB1*-TG mice. Microglial processes are like "sensors" of the brain microenvironment. The increased complexity of microglia processes in *ZEB1*-TG microglia may enable them to react more accurately and quickly to a stimulus. According to the gene array data, the terms affected by ZEB1 focus on immune system process and innate immune response. This confirms that microglial ZEB1 expression is involved in pathological immune responses following ischemic stroke.

The immune system participates in all stages in the aftermath of ischemic stroke, from the damage events to the regeneration processes (Iadecola and Anrather, 2011). In this context, reduced immune cell infiltration in the *ZEB1*-TG group in comparison with the WT group and neutrophils displayed the most obvious change. Neutrophils are known as crucial players during acute inflammation (Mantovani et al., 2011), and as pivotal immune components after ischemic stroke, neutrophils are one of the first cell types contributing to BBB disruption, edema, and neuronal death (Buck et al., 2008; Jickling et al., 2015). Infiltration of neutrophils into the ischemic area continues only 30 min post-stroke to several hours after ischemia peaks at 24–48 hr and then decline (Koh et al., 2015). Infiltrating neutrophils produce reactive oxygen species, cytokines, and metalloproteases, which aggravate tissue damage (Galli et al., 2011). The recruitment of neutrophils into tissue is orchestrated by tissue-resident cells, which could release multiple chemokines or adhesion molecules (Gelderblom et al., 2012; Kim and Luster, 2015; Strecker et al., 2017). In the CNS, astrocytes are the major source of CXCL1 in multiple animal models (Gelderblom et al., 2012; Rubio and Sanz-Rodriguez, 2007; Xu et al., 2014), which our results also confirmed. However, when we spatially separated astrocytes and neutrophils from either WT or *ZEB1*-TG mice that were cultured for 12 hr under OGD conditions, the migration index of neutrophils was similar for the two groups. Taken together, this suggests that *in situ* microglia might have been influencing the expression of CXCL1 in astrocytes. When we cultured astrocytes with *ZEB1*-TG microglia-conditioned medium, we discovered that CXCL1 was reduced compared with astrocytes alone; co-culture with WT microglia was similar. This suggests that *ZEB1*-TG microglia could regulate CXCL1 production in astrocytes.

With mammary carcinomas, TGF-β1 signaling can mediate the stromal-epithelial and host tumor interaction by regulating the expression of CXCL1 (Novitskiy et al., 2011). In the CNS, TGF-β1 is expressed primarily by microglia and, in association with invading macrophages, contributes to various forms of tissue damage (Kiefer et al., 1995; Lehrmann et al., 1995). On this basis, we reasoned that microglia and astrocytes might interact through the TGF-β1 pathway. The higher concentration of TGF-β1 in *ZEB1*-TG microglia might also explain why *ZEB1*-TG microglia maintain a less activated state after ischemic stroke (Butovsky et al., 2014). In this context, our overall results suggest that ZEB1 in microglia could affect the infiltration of neutrophils into the ischemic brain by regulating CXCL1 production in astrocytes through TGF-βRII. TGF-β1 is a prominent cytokine after stroke, reducing glial activation, suppressing the release of harmful oxygen- and nitrogen-derived products, and promoting angiogenesis in the penumbral area. On the other hand, TGF-β1 stimulates glial scar formation and amyloid production, which can lead to a higher risk of cognitive deficit (Ceulemans et al., 2010). Our experiment demonstrated another anti-inflammatory role of TGF-β1 during ischemic stroke. In the mouse TGF-β1

promoter region, there are three E2-box motifs for ZEB1 binding. Our promoter-reporter assay and ChIP assay results indicated that ZEB1 binds directly to the endogenous TGF-β1 promoter, resulting in the transcriptional activation of TGF-β1.

In summary, we revealed that ZEB1 is a key molecule in the regulation of microglia responses after brain ischemia. Its activity manifested through CNS microglia ameliorated the inflammatory burden after stroke by reducing the infiltration of neutrophils into CNS. This reduction is directly mediated by astrocytes through TGF-β1 signaling. Further understanding of ZEB1 function will aid in understanding how microglia contribute to the development of ischemic stroke. Manipulation of ZEB1 may provide a therapeutic opportunity for mitigating the consequences of ischemic stroke through modulation of microglia-mediated inflammation.

EXPERIMENTAL PROCEDURES

Mice

Mice carrying ZEB1-floxed alleles (Zeb1-TG and Zeb1-KD mice) were a gift from Dr. Shuang Yang, and CX3CR1^{CreER} mice were purchased from The Jackson Laboratory (#021160; Bar Harbor, ME, USA). For *in vivo* and *in vitro* experiments, 8-week-old male C57BL/6 mice and neonatal mice were used. All animal procedures were approved by the Animal Experiments Ethical Committee of Tianjin Medical University General Hospital.

Induction of Focal Cerebral Ischemia and Neurobehavioral Testing

Focal cerebral ischemia was modeled by inducing left-side tMCAO, based on the methods described by Longa et al. (1989). Then, neurological function was evaluated in each group of mice after tMCAO by using the mNSS, adhesive-removal test, foot-fault test, and corner-turning test (Li et al., 2017).

PCR

cDNA was prepared from cells or indicated tissues; primers are displayed in Tables S1, S2, and S3.

Immunohistochemistry

Immunohistochemistry staining was conducted as previously described (Li et al., 2017). See also the Supplemental Experimental Procedures.

Flow Cytometry

Single-cell suspensions were prepared from spleen or brain tissues and stained with fluorochrome-conjugated antibodies; more detailed information is given in the Supplemental Experimental Procedures.

In Vitro Cell Culture and Migratory Assay

Cells that were isolated were cultured under indicated conditions for migration as described previously (Jiang et al., 2017).

Statistics

Statistical analyses were performed using GraphPad Prism software. Differences were considered significant at $p < 0.05$. The Mann-Whitney U test was used to compare differences between groups. A one-way ANOVA followed by a Tukey *post hoc* test was used for three or more groups. Data are expressed as mean ± SEM.

DATA AND SOFTWARE AVAILABILITY

The accession number for the data reported in this paper is GEO: GSE110141.

SUPPLEMENTAL INFORMATION

Supplemental Information includes Supplemental Experimental Procedures, eight figures, and three tables and can be found with this article online at https://doi.org/10.1016/j.celrep.2018.03.011.

ACKNOWLEDGMENTS

This study was supported in part by the National Natural Science Foundation of China (81571600, 81322018, 81273287, 81100887, 81701193, and 81471535) and the Youth Top-notch Talent Support Program.

AUTHOR CONTRIBUTIONS

D.L. designed and performed experiments and wrote the manuscript; W.L., F.Z., and C.Z. performed specific experiments and analyzed data; C.W. revised the manuscript; Q.L. conceptualized the study and supervised the experiments; S.Y. provided essential reagents, technical guidance, and supervised the work; J.H. designed experiments and revised the manuscript.

DECLARATION OF INTERESTS

The authors declare no competing interests.

Received: November 13, 2017
Revised: February 10, 2018
Accepted: March 2, 2018
Published: March 27, 2018

REFERENCES

Ajami, B., Bennett, J.L., Krieger, C., Tetzlaff, W., and Rossi, F.M. (2007). Local self-renewal can sustain CNS microglia maintenance and function throughout adult life. Nat. Neurosci. *10*, 1538–1543.

Arnold, C.N., Pirie, E., Dosenovic, P., McInerney, G.M., Xia, Y., Wang, N., Li, X., Siggs, O.M., Karlsson Hedestam, G.B., and Beutler, B. (2012). A forward genetic screen reveals roles for Nfkbid, Zeb1, and Ruvbl2 in humoral immunity. Proc. Natl. Acad. Sci. USA *109*, 12286–12293.

Benakis, C., Garcia-Bonilla, L., Iadecola, C., and Anrather, J. (2015). The role of microglia and myeloid immune cells in acute cerebral ischemia. Front. Cell. Neurosci. *8*, 461.

Benarroch, E.E. (2013). Microglia: multiple roles in surveillance, circuit shaping, and response to injury. Neurology *81*, 1079–1088.

Buck, B.H., Liebeskind, D.S., Saver, J.L., Bang, O.Y., Yun, S.W., Starkman, S., Ali, L.K., Kim, D., Villablanca, J.P., Salamon, N., et al. (2008). Early neutrophilia is associated with volume of ischemic tissue in acute stroke. Stroke *39*, 355–360.

Bui, T., Sequeira, J., Wen, T.C., Sola, A., Higashi, Y., Kondoh, H., and Genetta, T. (2009). ZEB1 links p63 and p73 in a novel neuronal survival pathway rapidly induced in response to cortical ischemia. PLoS ONE *4*, e4373.

Butovsky, O., Jedrychowski, M.P., Moore, C.S., Cialic, R., Lanser, A.J., Gabriely, G., Koeglsperger, T., Dake, B., Wu, P.M., Doykan, C.E., et al. (2014). Identification of a unique TGF-β-dependent molecular and functional signature in microglia. Nat. Neurosci. *17*, 131–143.

Ceulemans, A.G., Zgavc, T., Kooijman, R., Hachimi-Idrissi, S., Sarre, S., and Michotte, Y. (2010). The dual role of the neuroinflammatory response after ischemic stroke: modulatory effects of hypothermia. J. Neuroinflammation *7*, 74.

Chaffer, C.L., Marjanovic, N.D., Lee, T., Bell, G., Kleer, C.G., Reinhardt, F., D'Alessio, A.C., Young, R.A., and Weinberg, R.A. (2013). Poised chromatin at the ZEB1 promoter enables breast cancer cell plasticity and enhances tumorigenicity. Cell *154*, 61–74.

Chamorro, Á., Dirnagl, U., Urra, X., and Planas, A.M. (2016). Neuroprotection in acute stroke: targeting excitotoxicity, oxidative and nitrosative stress, and inflammation. Lancet Neurol. *15*, 869–881.

Dagda, R.K., and Rice, M. (2017). Protocols for assessing mitophagy in neuronal cell lines and primary neurons. Neuromethods *123*, 249–277.

Fu, Y., Zhang, N., Ren, L., Yan, Y., Sun, N., Li, Y.J., Han, W., Xue, R., Liu, Q., Hao, J., et al. (2014). Impact of an immune modulator fingolimod on acute ischemic stroke. Proc. Natl. Acad. Sci. USA *111*, 18315–18320.

Fu, Y., Liu, Q., Anrather, J., and Shi, F.D. (2015). Immune interventions in stroke. Nat. Rev. Neurol. *11*, 524–535.

Funahashi, J., Sekido, R., Murai, K., Kamachi, Y., and Kondoh, H. (1993). Delta-crystallin enhancer binding protein delta EF1 is a zinc finger-homeodomain protein implicated in postgastrulation embryogenesis. Development *119*, 433–446.

Galli, S.J., Borregaard, N., and Wynn, T.A. (2011). Phenotypic and functional plasticity of cells of innate immunity: macrophages, mast cells and neutrophils. Nat. Immunol. *12*, 1035–1044.

Gelderblom, M., Weymar, A., Bernreuther, C., Velden, J., Arunachalam, P., Steinbach, K., Orthey, E., Arumugam, T.V., Leypoldt, F., Simova, O., et al. (2012). Neutralization of the IL-17 axis diminishes neutrophil invasion and protects from ischemic stroke. Blood *120*, 3793–3802.

Goldmann, T., Wieghofer, P., Müller, P.F., Wolf, Y., Varol, D., Yona, S., Brendecke, S.M., Kierdorf, K., Staszewski, O., Datta, M., et al. (2013). A new type of microglia gene targeting shows TAK1 to be pivotal in CNS autoimmune inflammation. Nat. Neurosci. *16*, 1618–1626.

Hasuwa, H., Ueda, J., Ikawa, M., and Okabe, M. (2013). miR-200b and miR-429 function in mouse ovulation and are essential for female fertility. Science *341*, 71–73.

Hu, X., Leak, R.K., Shi, Y., Suenaga, J., Gao, Y., Zheng, P., and Chen, J. (2015). Microglial and macrophage polarization—new prospects for brain repair. Nat. Rev. Neurol. *11*, 56–64.

Huang, W., Sherman, B.T., and Lempicki, R.A. (2009). Systematic and integrative analysis of large gene lists using DAVID bioinformatics resources. Nat. Protoc. *4*, 44–57.

Iadecola, C., and Anrather, J. (2011). The immunology of stroke: from mechanisms to translation. Nat. Med. *17*, 796–808.

Jiang, W., Li, D., Han, R., Zhang, C., Jin, W.N., Wood, K., Liu, Q., Shi, F.D., and Hao, J. (2017). Acetylcholine-producing NK cells attenuate CNS inflammation via modulation of infiltrating monocytes/macrophages. Proc. Natl. Acad. Sci. USA *114*, E6202–E6211.

Jickling, G.C., Liu, D., Ander, B.P., Stamova, B., Zhan, X., and Sharp, F.R. (2015). Targeting neutrophils in ischemic stroke: translational insights from experimental studies. J. Cereb. Blood Flow Metab. *35*, 888–901.

Kiefer, R., Streit, W.J., Toyka, K.V., Kreutzberg, G.W., and Hartung, H.P. (1995). Transforming growth factor-beta 1: a lesion-associated cytokine of the nervous system. Int. J. Dev. Neurosci. *13*, 331–339.

Kim, N.D., and Luster, A.D. (2015). The role of tissue resident cells in neutrophil recruitment. Trends Immunol. *36*, 547–555.

Kleinschnitz, C., Kraft, P., Dreykluft, A., Hagedorn, I., Göbel, K., Schuhmann, M.K., Langhauser, F., Helluy, X., Schwarz, T., Bittner, S., et al. (2013). Regulatory T cells are strong promoters of acute ischemic stroke in mice by inducing dysfunction of the cerebral microvasculature. Blood *121*, 679–691.

Koh, H.S., Chang, C.Y., Jeon, S.B., Yoon, H.J., Ahn, Y.H., Kim, H.S., Kim, I.H., Jeon, S.H., Johnson, R.S., and Park, E.J. (2015). The HIF-1/glial TIM-3 axis controls inflammation-associated brain damage under hypoxia. Nat. Commun. *6*, 6340.

Kriz, J., and Lalancette-Hébert, M. (2009). Inflammation, plasticity and real-time imaging after cerebral ischemia. Acta Neuropathol. *117*, 497–509.

Lehrmann, E., Kiefer, R., Finsen, B., Diemer, N.H., Zimmer, J., and Hartung, H.P. (1995). Cytokines in cerebral ischemia: expression of transforming growth factor beta-1 (TGF-beta 1) mRNA in the postischemic adult rat hippocampus. Exp. Neurol. *131*, 114–123.

Li, D., Wang, C., Yao, Y., Chen, L., Liu, G., Zhang, R., Liu, Q., Shi, F.D., and Hao, J. (2016). mTORC1 pathway disruption ameliorates brain inflammation following stroke via a shift in microglia phenotype from M1 type to M2 type. FASEB J. *30*, 3388–3399.

Li, M., Li, Z., Yao, Y., Jin, W.N., Wood, K., Liu, Q., Shi, F.D., and Hao, J. (2017). Astrocyte-derived interleukin-15 exacerbates ischemic brain injury via propagation of cellular immunity. Proc. Natl. Acad. Sci. USA *114*, E396–E405.

Longa, E.Z., Weinstein, P.R., Carlson, S., and Cummins, R. (1989). Reversible middle cerebral artery occlusion without craniectomy in rats. Stroke *20*, 84–91.

Macrez, R., Ali, C., Toutirais, O., Le Mauff, B., Defer, G., Dirnagl, U., and Vivien, D. (2011). Stroke and the immune system: from pathophysiology to new therapeutic strategies. Lancet Neurol. *10*, 471–480.

Mantovani, A., Cassatella, M.A., Costantini, C., and Jaillon, S. (2011). Neutrophils in the activation and regulation of innate and adaptive immunity. Nat. Rev. Immunol. *11*, 519–531.

Moskowitz, M.A., Lo, E.H., and Iadecola, C. (2010). The science of stroke: mechanisms in search of treatments. Neuron *67*, 181–198.

Murikinati, S., Jüttler, E., Keinert, T., Ridder, D.A., Muhammad, S., Waibler, Z., Ledent, C., Zimmer, A., Kalinke, U., and Schwaninger, M. (2010). Activation of cannabinoid 2 receptors protects against cerebral ischemia by inhibiting neutrophil recruitment. FASEB J. *24*, 788–798.

Nimmerjahn, A., Kirchhoff, F., and Helmchen, F. (2005). Resting microglial cells are highly dynamic surveillants of brain parenchyma in vivo. Science *308*, 1314–1318.

Novitskiy, S.V., Pickup, M.W., Gorska, A.E., Owens, P., Chytil, A., Aakre, M., Wu, H., Shyr, Y., and Moses, H.L. (2011). TGF-β receptor II loss promotes mammary carcinoma progression by Th17 dependent mechanisms. Cancer Discov. *1*, 430–441.

Parkhurst, C.N., Yang, G., Ninan, I., Savas, J.N., Yates, J.R., 3rd, Lafaille, J.J., Hempstead, B.L., Littman, D.R., and Gan, W.B. (2013). Microglia promote learning-dependent synapse formation through brain-derived neurotrophic factor. Cell *155*, 1596–1609.

Rubio, N., and Sanz-Rodriguez, F. (2007). Induction of the CXCL1 (KC) chemokine in mouse astrocytes by infection with the murine encephalomyelitis virus of Theiler. Virology *358*, 98–108.

Stevens, B., Allen, N.J., Vazquez, L.E., Howell, G.R., Christopherson, K.S., Nouri, N., Micheva, K.D., Mehalow, A.K., Huberman, A.D., Stafford, B., et al. (2007). The classical complement cascade mediates CNS synapse elimination. Cell *131*, 1164–1178.

Strecker, J.K., Schmidt, A., Schäbitz, W.R., and Minnerup, J. (2017). Neutrophil granulocytes in cerebral ischemia - Evolution from killers to key players. Neurochem. Int. *107*, 117–126.

White, G.E., and Greaves, D.R. (2012). Fractalkine: a survivor's guide: chemokines as antiapoptotic mediators. Arterioscler. Thromb. Vasc. Biol. *32*, 589–594.

Wieghofer, P., Knobeloch, K.P., and Prinz, M. (2015). Genetic targeting of microglia. Glia *63*, 1–22.

Xu, J., Zhu, M.D., Zhang, X., Tian, H., Zhang, J.H., Wu, X.B., and Gao, Y.J. (2014). NFκB-mediated CXCL1 production in spinal cord astrocytes contributes to the maintenance of bone cancer pain in mice. J. Neuroinflammation *11*, 38.

Yona, S., Kim, K.W., Wolf, Y., Mildner, A., Varol, D., Breker, M., Strauss-Ayali, D., Viukov, S., Guilliams, M., Misharin, A., et al. (2013). Fate mapping reveals origins and dynamics of monocytes and tissue macrophages under homeostasis. Immunity *38*, 79–91.

Zhang, P., Wei, Y., Wang, L., Debeb, B.G., Yuan, Y., Zhang, J., Yuan, J., Wang, M., Chen, D., Sun, Y., et al. (2014). ATM-mediated stabilization of ZEB1 promotes DNA damage response and radioresistance through CHK1. Nat. Cell Biol. *16*, 864–875.